

Development of a Relative Positioning System for Mobile Robots

Raphaël Cherney

Semester Project
Fall 2011



ÉCOLE POLYTECHNIQUE
FÉDÉRALE DE LAUSANNE



Professor: Auke Jan Ijspeert
Assistant: Alessandro Crespi

Abstract

This report presents the design of a relative positioning system for mobile robots that uses modulated infrared or visible light to determine the range and direction to a modulated source. Prototype hardware was designed, assembled, and tested to demonstrate the system. The sensor is insensitive to ambient light differences and other environmental factors. The system allows for low bandwidth communication between a source and receiver and can also be used to detect obstacles (using an onboard transmitter). The device is smaller than existing systems, and be easily adjusted to suit new environments.

Contents

1	Introduction	4
1.1	Background	4
1.2	Project goals	4
2	State of the art	5
2.1	Existing components	5
2.2	Underwater sensors	5
2.3	Mobile robot relative positioning	6
3	System design	6
3.1	Operating principle	6
3.1.1	Distance estimation	7
3.1.2	Direction determination	8
3.1.3	Communication	9
3.2	Transmitter	10
3.3	Receiver	11
3.4	Photodetector	12
3.5	Signal selection	14
3.6	Cascaded filter chain	14
3.7	Level detector	15
3.8	Microcontroller	16
3.9	Simulation	17
4	Hardware	18
4.1	First prototype	19
4.2	Second prototype	20
5	Results	20
5.1	Distance calibration	20
5.2	Angle determination	22
5.3	Reflective obstacle sensing	22
5.4	Communication	22
6	Conclusion and future work	23
A	Schematics	28
B	Printed circuit board	32
C	Datasheets	33
C.1	TSKS5400	33
C.2	TEKT5400	33
C.3	CD74HC4052	33
C.4	TLV2774/2	33
C.5	BAS16	33
C.6	2N7002	33

1 Introduction

1.1 Background

There are many situations in which knowing one's position relative to another point is useful. Such a reference can aid in navigation or provide other useful information – especially in cases where a global reference frame is unimportant. In the field of mobile robotics, having a sensor which simply determines the range and bearing of a transmitter opens up a wide variety of possible behaviors and research scenarios. In many cases the transmitter is fixed, but in others, such as with collective robotic systems, the transmitter can move and have some level of associated intelligence. Systems that enable relative localization are often complex, large, and expensive. However, taking advantage of commonplace technologies such as components from infrared communication systems, we can create simple, miniature, and low-cost solutions.

The Biorobotics Laboratory at the École Polytechnique Fédérale de Lausanne (EPFL) has a variety of biologically-inspired robotic systems. In order to enable more autonomous motion of robots (and the *Salamandra robotica* [17] in particular), the robots must be able to get a better sense of the environment around them. This would ideally be done with onboard sensors and would be robust to various environmental conditions (lighting, temperature, water, etc.). This project investigates the creation of a relative positioning system that leverages existing technologies and designs to create a solution which allows robots to find, track, and communicate with known sources. In particular, using modulated light allows the system to be used in a much wider variety of environments. Examples of scenarios include autonomous robotic salamanders looking for (or avoiding) various beacons in the environment (see Figure 1) or multiple robots attempting to coordinate their motion.



Figure 1: Conceptual image showing a robotic salamander moving towards a beacon.

1.2 Project goals

This project entails the creation of an novel relative positioning system for mobile robots. In particular, we hoped to use modulated infrared signals to determine the distance and direction of an active modulated sender, decode data sent by the sender (e.g. an 8-bit ID transmitted a few times per second), and study the possibility of using the same sensor (by adding some transmitter) for obstacle sensing. Since the system was to be used with the *Salamandra robotica* platform, the sensor should also be small, lightweight, waterproof, and powered by onboard supplies. This design process was to include a state of the art survey, the design of the system, and the implementation of a functioning

prototype. Ultimately, such a system can be integrated into the robot and enable more autonomous behaviour.

2 State of the art

Infrared light is a common, easy-to-use, low power, and low-cost way to transmit information. Because of this, there are a wide range of systems that have been developed that use this technology for wireless communication, object detection, and other tasks. Due to high attenuation of infrared radiation in underwater communication, a lot of research has been done to investigate alternative communication channels, namely using visible light. Recently, with the advancement of mobile robotics, more application-specific examples have arisen, namely in the realm of proximity sensing and localization. We begin by reviewing available components and the state of the art for relative localization and communication systems. This background informs the design of our system (which is presented in Section 3).

2.1 Existing components

There are a wide range of components available for creating infrared and optical channels. In particular infrared and visible LEDs, photodiodes, and phototransistors are extremely common and low-cost. Infrared is also widely used as a local wireless network medium. Most devices using this technology follow the standards set up by the Infrared Data Association (IrDA). These common guidelines allow for a wide range of dissimilar devices to communicate and work together. Most infrared communication devices are focused on maximizing data rates while minimizing errors and are less concerned with signal strength and localization. Because most commercially available devices are highly integrated, they are also particularly hard to adapt to different applications. In fact, extracting additional (analog) information can be nearly impossible for many systems. A few exceptions do exist. For example, the TSOP4P series of infrared receiver modules output analog signal information in the form of a pulse width of varying length linked to the time it takes the AGC to suppress a quasi continuous signal. The output pulse width is linearly related to the irradiance. The devices use modulated infrared light (and thus have the benefits of rejecting ambient light signals) and are highly integrated, easing integration. If the adaptability of the system is less important, communication could be deprecated, and a smaller dynamic range is required, these components could provide a simple solution.

2.2 Underwater sensors

Water absorbs light at infrared wavelengths much more readily than it does blue/green light. For this reason, several researchers have been looking toward new or adapted systems that can perform better underwater. Essentially all of these applications, however are more of an extension of infrared communication technology to the underwater environment. Because of this, there is still a lack of components taking advantage of analog information contained in signal. Nevertheless, these examples show how to use existing technologies to create systems that can work in a wider range of environments. [3] provides a good overview of advances in the field. In terms of using visible light to communicate, most sources agree that we can achieve better performance using blue/green light as observed in [4], however Tivey points out in [62] that while blue wavelengths

theoretically suffer less attenuation underwater than infrared wavelengths, blue light is more strongly scattered by particulates and minute bubbles in the water than red light. Furthermore, silicon detectors are twice as sensitive to red light than to blue light. These factors makes it so that blue and green light are not always advantageous when compared to red or infrared light in water.

2.3 Mobile robot relative positioning

Multirobot systems are a growing field of research that offers the prospect of considerable advantages when compared to single-robot systems (e.g. simultaneous sensing and acting, reconfigurability, redundancy, etc.). Many of these advantages, however, only come when the robots have a relative sense of position. Motivated by these goals, the field of mobile robotics has several recent examples of successful relative positioning and communication systems. Most of these devices are a little too large to fit on the *Salamadra robotica* but are good ideas to base our design on. [34], [49], and [23] all present good examples of such systems. There are a few common themes to these designs. Namely, they use the signal strength to estimate range and use an array of rotated detectors array to estimate bearing (taking advantage of the declining sensitivity of receivers with respect to the receiving angle). A recent, notable example of such a system is the Range and Bearing Infrared Transceiver (RABIT), presented in [53]. This system for miniature aerial vehicles (MAVs) had similar design constraints and goals, and it is able to achieve these impressive results through the use of a novel cascaded filter chain to perform the signal strength measurement. This, and other mobile robot designs heavily influenced the design presented in the following section.

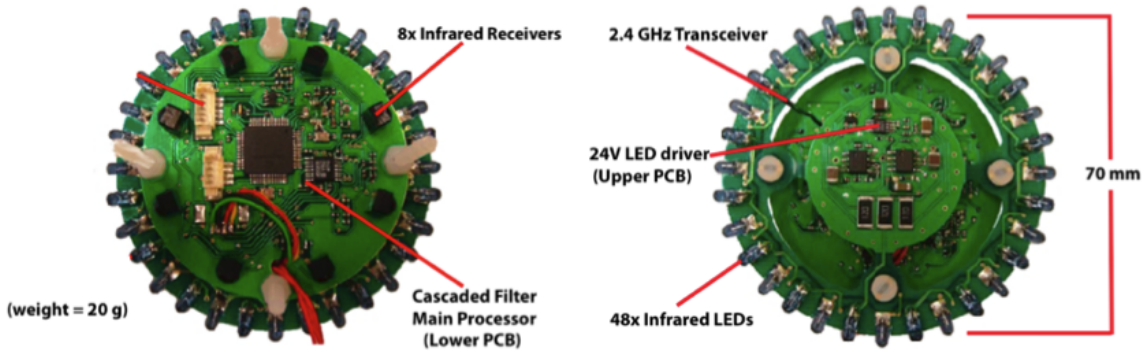


Figure 2: The Range and Bearing Infrared Transceiver (RABIT) [53].

3 System design

3.1 Operating principle

Much like most other relative positioning systems in mobile robots, the proposed design uses a detector array which determines the distance and direction of an incoming signal based on the total and relative signal strengths for each receiver. The detectors are only sensitive to particular frequencies and wavelengths which are matched between the transmitter and receiver. In addition, the proposed design includes an onboard transmitter, allowing for communication from the robot and enabling the detector array to be used for

obstacle detection. In this case, light from the onboard transmitter is reflected off of an obstacle and identified (much like any other source) by the sensor. Figure 3 shows a the approximate position and sensitivity of the sensors on the head of the robot, in addition to the relative transmitter intensities of three onboard transmitters.

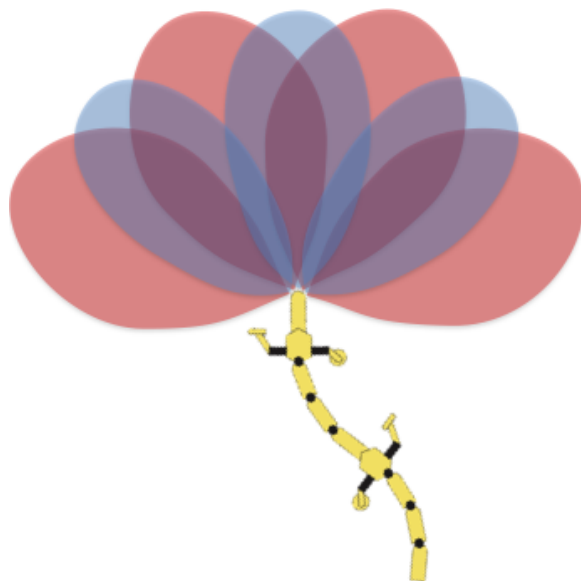


Figure 3: Diagram showing approximate sensitivity of the four receivers (in red) and coverage of the onboard transmitters (in blue).

3.1.1 Distance estimation

All emitters of visible and infrared light distribute their energy over some area. As one moves away from the source, the energy received in a given area (i.e. a detector) drops off as a function of the square of the distance. That is to say, even though the total power projected by a emitter remains the same, the energy is distributed over a larger area the farther one moves away from the source. This drop off rate (as shown in 4) is well known and consistent. This implies that if we know the power of the transmitter and signal level at the receiver, we can estimate the distance between the two. In our case, we assume an even coverage of emitted light coming from the transmitter (i.e. the intensity of the signal is not dependent on the angle of the transmitter). This assumption holds if there are sufficient transmitters to account for variations in individual transmission intensity and angular variations. We also assume a single signal source and a known or negligible absorption by the transmission medium. In particular, we can calibrate the sensor for differences between transmission through air and water. To measure the baseline signal strength, we also assume perfect alignment of the receiver with the transmitter.

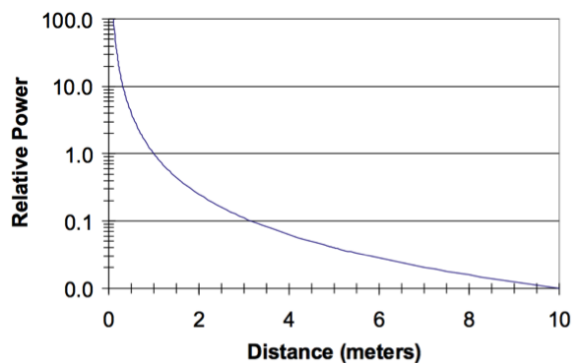


Figure 4: Graph showing the typical decrease in received power (signal strength) with respect to distance (from [8]).

Normally measurements based on signal strength would be greatly affected by the ambient light level. The proposed system, however, only considers the signal strength for signals at the proper modulated frequency and wavelength. This fact allows us to separate the controlled source light from different environmental conditions, allowing for use in a wide variety of environments.

3.1.2 Direction determination

Using multiple receivers allows us to gather more information from the incoming signal. In particular, receivers will have varying sensitivities depending on the angle of the incoming signal relative to the orientation of the detector. If the detectors are arranged such that there is an overlap in their sensitive regions, we can consider the relative strengths of the received signals for each detector to estimate the direction of the transmitter.

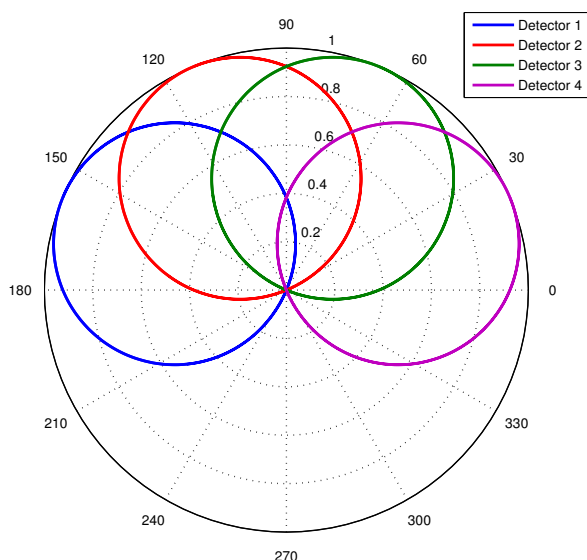


Figure 5: Polar plot showing the overlap in angular sensitivity assuming an angular strength profile of $r' = r \cos(\theta)$.

A wide variety of algorithms exist to extract the range and bearing information from an array sensors in a known geometry. In the simplest case, we can simply define the angle

of the incoming signal as the angle of the detector with the strongest signal. This method is considerably more effective when the number of receivers is increased, but it can always be improved by considering inputs from the neighboring sensors. One can then interpolate between several detector readings to get a better estimate of bearing. Pugh and Martinoli propose in [49], an algorithm to extract both distance and bearing information from signal strength measurements of a series of evenly-spaced receivers. In particular, if we assume that the angular reception strength profile is given by $r' = r \cos(\theta)$, a reasonable model for our receivers, we can find the distance and bearing by the following equations:

$$r = \frac{1}{\sqrt{a^2 + b^2}} \quad (1)$$

$$\theta = \arctan\left(\frac{b}{a}\right) + Q \quad (2)$$

with

$$a = \frac{r^L + 2r^M + r^R}{2 \cos\left(\frac{\pi}{4}\right) + 2} \quad b = \frac{r^L - r^R}{2 \sin\left(\frac{\pi}{4}\right)} \quad (3)$$

where r is the calculated distance to the source, θ is the calculated angle to the source relative to the detector with the strongest response, r^M is the distance measurement from the detector with the strongest signal (shortest range), r^L and r^R are the distance measurements from the detectors to the left and right of r^M , and Q is 2π if θ is negative (zero otherwise).

3.1.3 Communication

There are many different methods to communicate over the optical channel we create. Typically, modulation techniques are selected for power efficiency, bandwidth efficiency, and other considerations (such as simplicity). In this case, data rates are less important than being able to determine the location of the transmitter. We are therefore willing to sacrifice power efficiency to ensure more consistent position readings. More advanced discussion of modulation techniques can be found in [22] and [32]. Some basic ideas we played with were the following:

On-off keying (OOK) OOK is the simplest and most common form of optical communication. A bit value of one is represented by an optical pulse that occupies the entire bit duration while a zero bit is represented by the absence of a signal.

Pulse width modulation (PWM) Information is encoded in the duty cycle of a PWM signal.

Pulse position modulation (PPM) PPM a very commonly used baseband modulation technique. It is what IrDA uses. It consists of a signal pulse (either on or off) in the slot corresponding to the particular bit, with the rest of the slots being the opposite.

Digital pulse interval modulation (DPIM) In DPIM, the information is encoded in the amount of time between a pulse (either high or low).

3.2 Transmitter

A key component of the proposed relative positioning system is the transmitter. The transmitter is responsible for outputting a modulated (10 kHz) signal with a constant power level during transmission and must have the ability to turn on and off transmission at the appropriate time depending on the digital modulation method used to transfer data. It is important that the signal strength is nearly uniform regardless of the transmitter's orientation so that the receiver can get a consistent and precise distance measurement.

Ideally the design would be simple, adaptable, and use few components. Figure 6 shows quite possibly the simplest circuit to accomplish this goal. It consists of an LED, resistor, and transistor switch in series. The LED should be chosen to match the design and power requirements of the system. In particular, the wavelength, switching speed, irradiation profile, and power output should be considered to ensure adequate range. With a sufficiently high voltage supply, multiple LEDs can also be placed in series. The resistor should be selected to create an appropriate transmitting current based on the properties of the LED emitter. Note that the physical resistor should also have an adequate power rating. Finally, a transistor switch (such as an n-channel MOSFET) can be used to create the modulated signal based on the output from a microcontroller. Using a transistor instead of simply driving the LED from the microcontroller output pin allows for higher currents (and therefore longer ranges). The transistor should be able to pass the necessary currents to drive the circuit. In most cases, multiple emitters should be used to create a uniform emission from the transmitter. This can be done by replicating the proposed circuit multiple times in parallel (using the same output signal). It is best to ensure adequate overlap between adjacent transmitters to create a nearly uniform output profile.

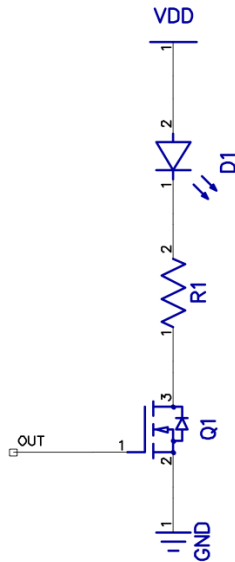


Figure 6: Simple transmitter circuit. An oscillating OUT signal that turns the emitter on and off at the desired frequency.

One of the best design features of this circuit is its adaptability. A wide range of emitters, both infrared and visible, can be used to transmit the signal. In fact, almost any kind of light emitting diode can be used, assuming an adequate supply voltage, an appropriate

resistor choice, and a transistor which can pass sufficient current. For the implementation used in the prototypes, the circuit uses an 5V supply from the robot. Several LEDs were used during testing, but the final prototype contains three TSKS5400 infrared LEDs. These emitters, when installed with $\frac{\pi}{4}$ angular separation, have a combined output profile which is approximated in Figure 7. While it is far from being perfectly uniform, given the small number of components used, it functions as an adequate transmitter prototype. Three 2N7002 n-channel MOSFETs were used as switches. These small devices can pass 300 mA of DC current, more than adequate for a wide range of low-power emitters. Note that the range of the device can be increased by increasing the power output of the transmitter (and calibrating appropriately). A 5 meter range is definitely possible with such a design; however the transmitter would require a sufficient power supply and several, powerful LEDs. The prototype system simply uses the low-power, onboard transmitter from a second board to act as a transmitting source.

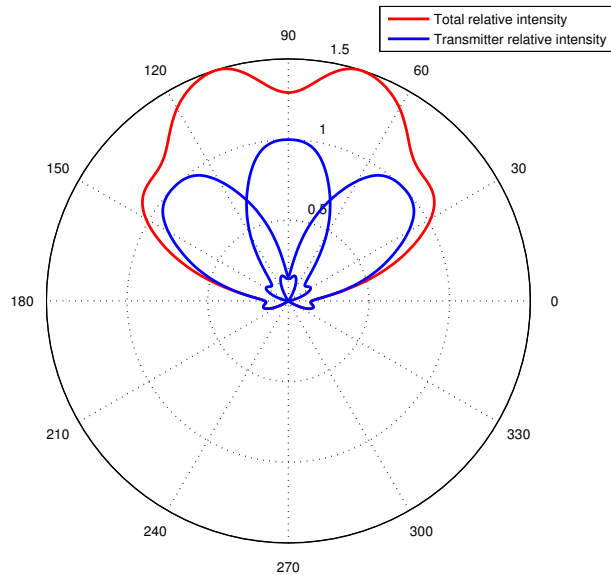


Figure 7: Graph showing the published angular intensity of three TSKS5400 infrared transmitters with $\frac{\pi}{4}$ angular separation (in blue) and the total emitted intensity (in red).

3.3 Receiver

The receiver itself consists of several parts. There is a detector array, analog multiplexer, cascaded filter chain, series of peak detectors, and finally a microcontroller to monitor signals and interface with the robot. Figure 8 shows a block diagram of how all of the parts are connected.

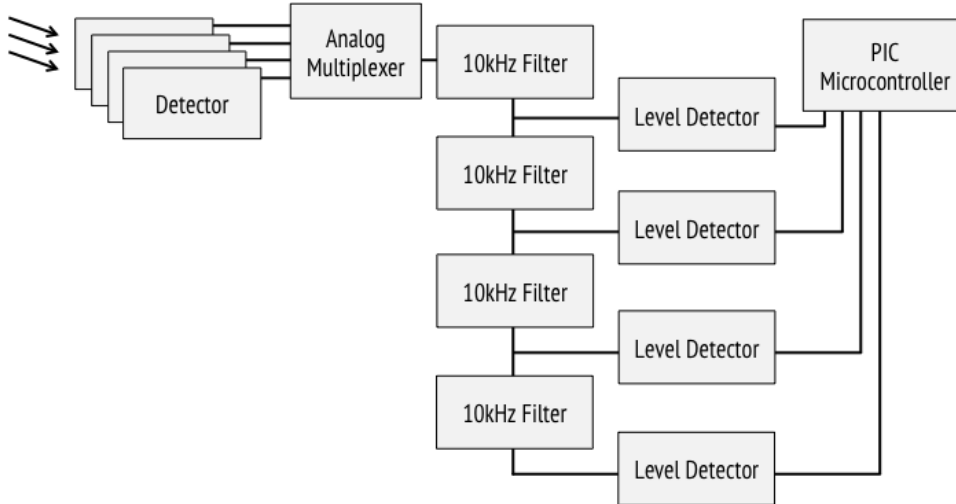


Figure 8: Block diagram showing the setup of the receiver circuitry.

3.4 Photodetector

Light from the transmitter travels through space and is received by a photodetector. The amount of light measured by the photodetector is inversely proportional to the distance from the transmitter. Photodiodes and phototransistors are the most common detectors of infrared and visible light signals. These devices can convert light energy into current signals. A photodiode is similar to a standard diode except that it is packaged in a way to allow light to strike the PN junction. This light energy creates electron-hole pairs, creating in a photocurrent which is proportional to the amount of incoming light. The cases around these devices often act as both a lens to capture more light and a filter to eliminate unwanted wavelengths. Phototransistors use similar physics but amplify the light signal by the β of transistor, resulting in a significantly higher sensitivity. This, however, comes at the cost of a slower response time (phototransistors typically have t_{on}/t_{off} of $2 \mu\text{s}$ or more [8]). Photodetectors are typically operated in reverse bias. Note that sensitivity can be increased by operating multiple photodetectors in parallel.

In order to work more easily with the signals from photodetectors, it is useful to convert the signal to a voltage and amplify it. There are many methods of creating a voltage signal with a photodetector, several of these are shown in Figure 9. The simplest design is to connect a terminating resistor and use the fact that $V = I_{photo}R$. Depending on the detector sensitivity and resistor value, this can provide an adequate result. This solution, however, suffers from a relatively small dynamic range when we consider the range of currents we need to measure. In order to increase the dynamic range, we can use multiple terminating resistors which can be selected by different transistor switches (controlled by an external element). This signal can then be sent to a preamplifier, amplified, and filtered. There is a risk, however, that the preamplifier will have difficulty with signals at the extremes of the power supply – which can be very likely when using a simple terminating resistor. A very common circuit structure used in these cases, which integrates the amplification directly, is the transimpedance amplifier. This well-known current-to-voltage converter is usually connected directly to the current source, but if we AC-couple the detector instead, we can effectively eliminate the DC ambient light signal at the source. Figure 9c shows the transimpedance amplifier circuit used in the final prototype. The DC signal is passed through R1, while the modulated AC signal is passed

through C1 and amplified.

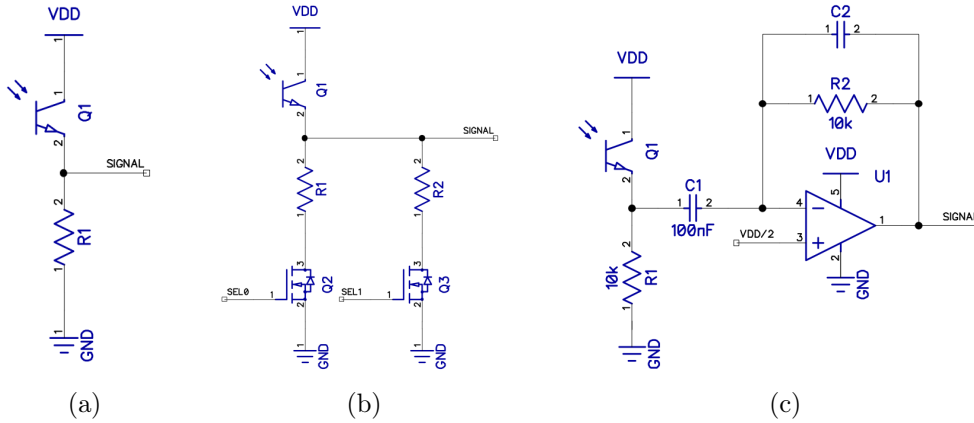


Figure 9: Three detector circuit designs.

For our prototype implementation, we chose to use the AC-coupled transimpedance amplifier. It filters out the ambient light directly, amplifying only the signals of interest. It is also compact and easily adjustable. It can be used with many standard photodiodes or phototransistors, and the amount of amplification can be changed with a single resistor. This greatly increases the versatility of the circuit. The final boards use four TEKT5400S phototransistors as the detectors. They are in a small array with a difference of $\frac{\pi}{4}$ between each detector. Figure 10 shows the relative angular sensitivity of these sensors (using published angular reception strength profiles). The overlap of the sensitive regions and known angular sensitivity profiles allows us to estimate the distance and angle of signals between two detectors.

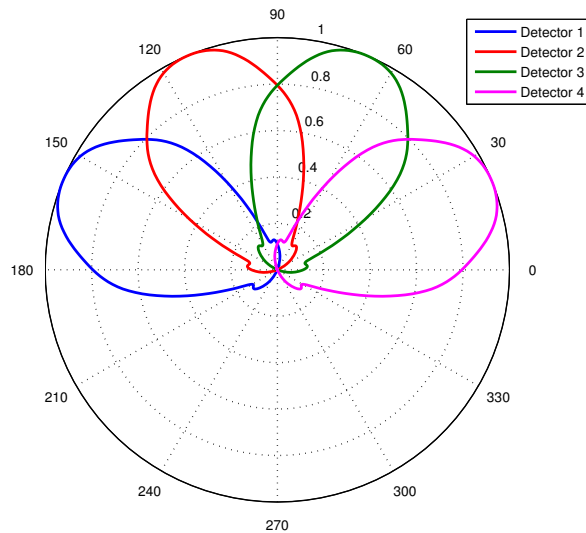


Figure 10: Polar plot showing the published relative angular sensitivity of four TEKT5400S phototransistors with $\frac{\pi}{4}$ angular separation.

3.5 Signal selection

The proposed receiver uses an array of photo-sensitive detectors. Each detector has its own associated signal. In order to make efficient use of the filters, it is best to use a single cascaded filter chain and simply change which signal is being measured. This can be done using a variety of different components. Solid-state components typically give faster switching times and more resilient operation. In this case, we can use a series of analog switches (as used in the first prototype) or an analog multiplexer (as in the second prototype). Analog multiplexers have the advantage of guaranteed break-before-make switching, ensuring multiple preamplifiers are not connected (causing interference), even for a short period. The final prototype uses a CD74HC4052 analog multiplexer which features a low ON resistance of 70Ω , low crosstalk between channels, and an practically no feedthrough at 10 kHz (-100 dB).

3.6 Cascaded filter chain

One of the more unique aspects of the proposed system is the cascaded amplifying filter chain. This design choice, inspired by [53], allows us to dramatically increase the dynamic range of our sensor. We are able to achieve large amplifications (1000x) while maintaining good stability (the amplification is divided into multiple stages, each with a gain of 10) and accessibility of the range information (signal can be read after each stage). Furthermore, because each stage acts as a band-pass filter, we create a progressively sharper filter (8th order by the 4th stage). The design is compact and has a high sensitivity to the desired frequency. Alternative designs of dynamically changing the amplification are typically larger, more complex, and more prone to instability.

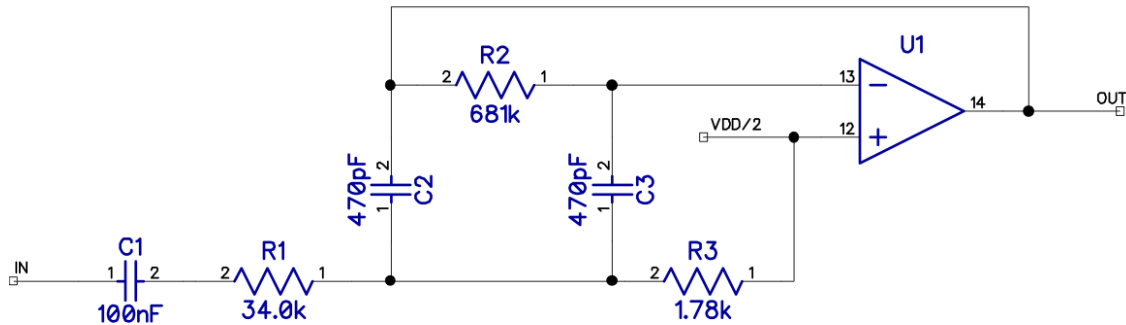


Figure 11: A 10 kHz active, amplifying band-pass filter (modified Deliyannis filter). Four of these circuits are connected in series to achieve greater signal separation and amplification.

The filter circuit used in the prototype is a modified Deliyannis filter topology. It runs on a single supply and uses a single operational amplifier and only 5 components (plus an AC-coupling capacitor), keeping the design simple and compact. Figure 11 shows the single supply circuit schematic. The Q is set at 10, locking the gain at 10, as the two are related by $Q = Gain = \frac{R2}{2 \cdot R1}$. A higher Q is not used because the operational amplifier gain bandwidth product can be easily reached, even with a gain of 20 dB. The prototype uses a 10 kHz carrier, chosen because it is not a common frequency in testing

environments (low noise) and does not require specific high-frequency hardware (most emitters, detectors, and filters work well at this frequency). The simulated frequency response of the 10 kHz filter is shown in Figure 12. The filter can be adapted to suit other carrier frequencies by simply changing the passive component values according to the following equations:

$$\begin{aligned}
 C1 &= 100 \cdot C2 \text{ to } 1000 \cdot C2 \text{ (not critical)} \\
 C2 &= C3 \\
 R1 &= \frac{1}{2\pi \cdot C2 \cdot \text{frequency}} \\
 R2 &= 20 * R1 \\
 R3 &= \frac{R1}{19}
 \end{aligned} \tag{4}$$

The prototype hardware uses TLV2774 quad operational amplifiers. These devices feature single-supply, rail-to-rail output operation with a slew rate of $10.5 \text{ V}/\mu\text{s}$ and a gain-bandwidth product of 5.1 MHz at 5 V. These devices are more than sufficient for the application. In general, the operational amplifier should have a sufficient slew rate to allow a 5 V peak-to-peak 10 kHz sine wave. An low-cost, alternative device is the MCP6004, a quad 1 MHz rail-to-rail operational amplifier.

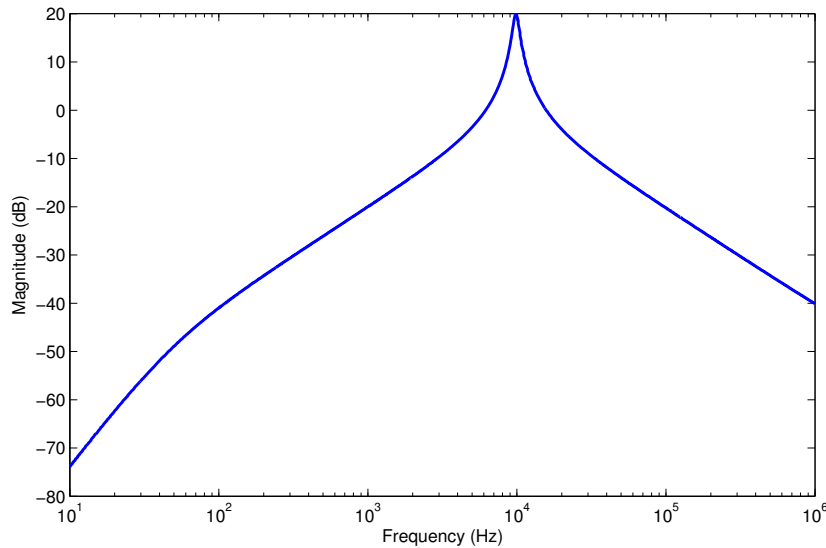


Figure 12: Simulated frequency response of the filter.

3.7 Level detector

The output from the filters are 10 kHz signals of differing amplitudes. Unfortunately, these high frequency signals are too fast for the analog-to-digital converter (ADC) on PIC18 microcontrollers. The typical solution is to measure the peak voltage of the signal (a constant input) to capture the signal strength. Figure 13 shows several peak detector circuits. Quite possibly the simplest peak detector consists of a simple signal diode and a grounded capacitor (Figure 13a). The highest point of the input waveform charges the capacitor, which holds the voltage while the diode is reverse-biased. This circuit, while simple, has several disadvantages. It has a variable input impedance (which is particularly low during the peaks) and the diode drop makes it inaccurate by one diode drop (and completely insensitive to peaks under one diode drop). A better circuit is

shown in 13b. This circuit uses an operational amplifier to introduce feedback into the circuit, eliminating the diode drop. This circuit will hold the actual peak value as long as it is below one diode drop below VDD (the op amp saturates). This circuit should use a low-leakage diode and an op amp with a low bias current and sufficient slew rate. The final circuit in Figure 13 shows an advanced peak detector which eliminates the diode leakage by adding another feedback layer, further improving the result. Unfortunately, resetting the peak measurements is more complicated for this circuit and requires a transistor switch or leakage resistor.

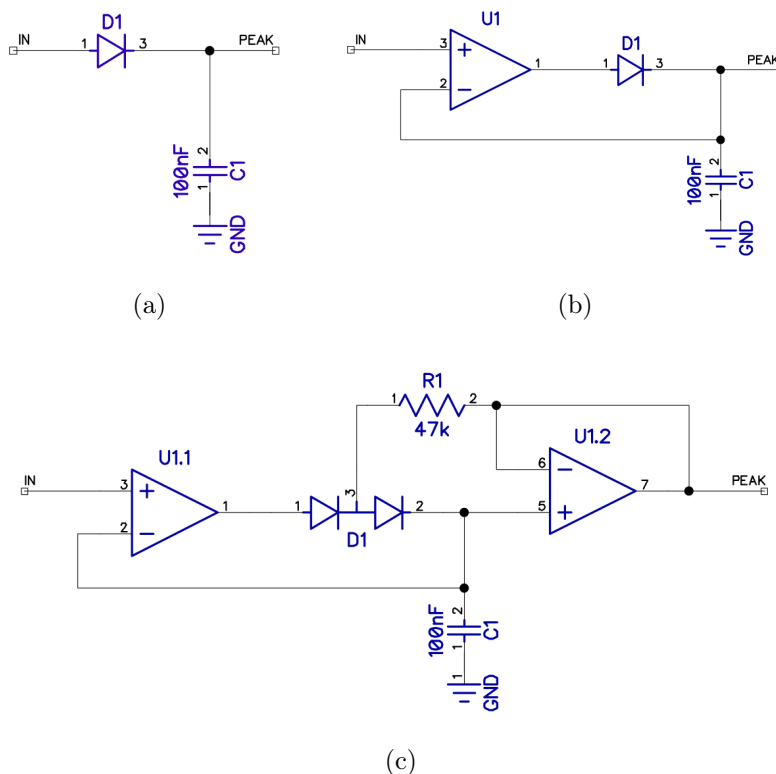


Figure 13: A series of simple peak detector circuits.

The prototype hardware uses the circuit in Figure 13b because it can be easily reset without further hardware by quickly changing the microcontroller input pin to an output source and momentarily pulling it low before reconfiguring the pin as an input. Note that, because the input signal is centered around $V_{DD}/2$, the output of the peak detectors will always be between $V_{DD}/2$ and one diode drop below VDD. Something that was not done in the prototype circuits, but may be desirable in later designs would be to AC-couple the peak detector and shift the signal to another level to make analog to digital conversions more convenient.

3.8 Microcontroller

All of the low-level control signals, analog-to-digital conversions, data processing, and external interfacing are handled by a PIC18 microcontroller. These small, low-power devices are highly flexible and include a range of built-in hardware peripherals, including a 10-bit analog-to-digital converter (ADC). The prototype hardware uses the PIC18F2580, which

was picked for its existing use throughout the Biorobotics Laboratory. The microcontroller was programmed in C using C18 compiler and the MPLAB integrated development environment. The prototypes include standard connectors to interface with Microchip’s programmers and debuggers (a PICkit3 was used for testing). The prototype hardware runs off of a 5 V supply (provided by the robot or external source) and uses a external oscillator to create a 20 MHz clock. The sensor communicates through a serial connection to the robot or a computer (aided by an external FTDI chip). In order to improve the ADC reading, external voltage references can be used (SOT23 package).

3.9 Simulation

In order to verify the design, the circuit was modeled using the LTspice IV simulation environment. SPICE models were provided by the manufacturers whenever possible, and a number of test circuits were created. Figure 14 shows the simulated output from the detector circuit, modeling the photodiode as a current source (10 nA, 10 kHz square wave) along with 1-2 uA 60 Hz noise. The output of each stage of the cascaded filter chain is in Figure 15. Finally, Figure 16 shows the simulation results for the peak detector circuit (using a n-channel MOSFET to reset the peak voltage).

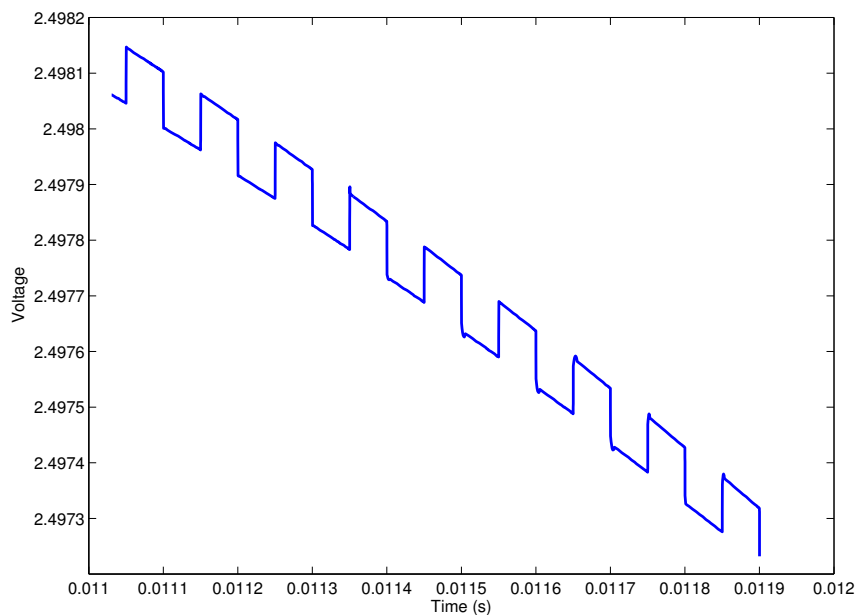


Figure 14: Graph showing the simulated output from the detector circuit with a 10 nA signal and large 60 Hz noise.

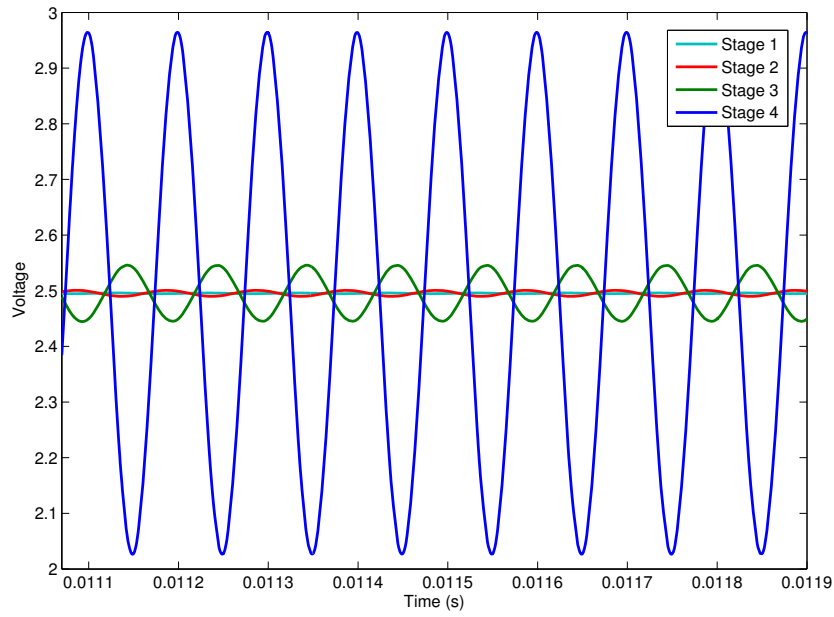


Figure 15: Graph showing the simulated output after each stage of the filter chain.

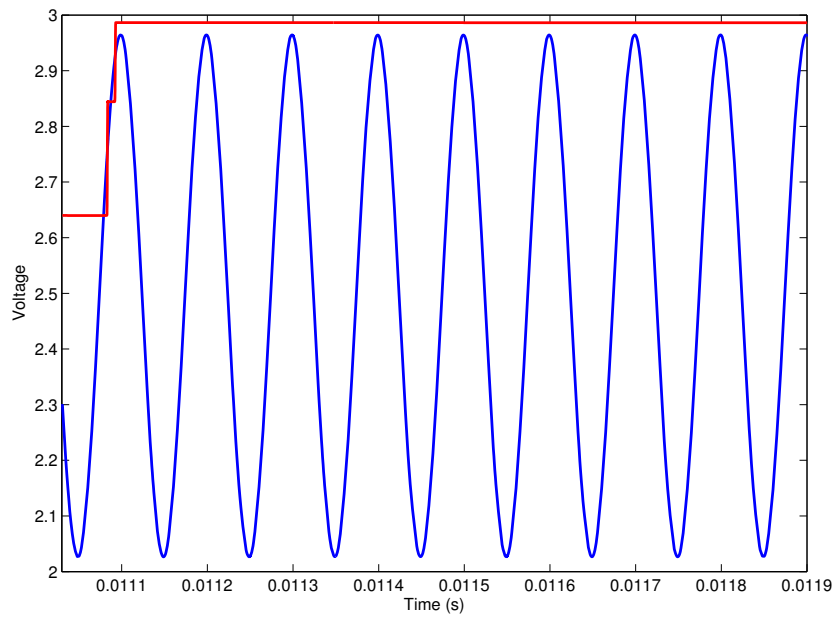


Figure 16: Graph showing the simulated output of the peak detector circuit.

4 Hardware

Prototype hardware was created and tested to verify the system design. This involved several steps including component selection, schematic design, PCB layout, manufacturing, and testing. The designs use only off-the-shelf electrical components, reducing

the cost and increasing the ease of replication. This section briefly describes the two prototypes that were built.

4.1 First prototype

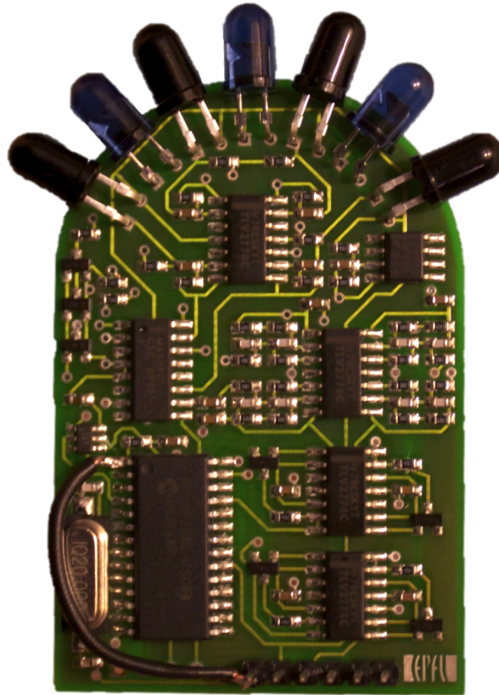


Figure 17: First prototype of transceiver.

After designing and simulating the circuit, we ran several quick tests with infrared emitters and receivers using solderless breadboards. This provided some insight into the basic activity we could expect, but we needed a more refined circuit to do more advanced testing (particularly of the filters). We opted to create a prototype printed circuit board (PCB) transceiver to test the analog circuit, prototype the firmware, and catch design errors. The first revision of the sensor integrated both the transmitter and receiver into a single transceiver. The transceiver used a semicircle of 4 detectors and 3 emitters ($\frac{\pi}{8}$ angular separation alternating between receiver and transmitter). The outputs from the detectors were passed through an analog switch (MAX392) and into the cascaded filter chain. Peak detectors as described in Figure 13c were used after each of the filter stages. Peak voltages were passed to the PIC microcontroller for readout.

Testing of this circuit showed very good correlation with the simulation results. In particular, oscilloscope readings at intermediate points showed nearly identical behavior to what is seen in section 3.9. Testing was done using several emitters and detectors, using both infrared and visible light. All wavelengths tested returned functionally equivalent results (using matched detectors and emitters). Using a function generator and single LED emitter, the range was briefly tested, showing detectable signals at ranges exceeding 4 meters.

4.2 Second prototype

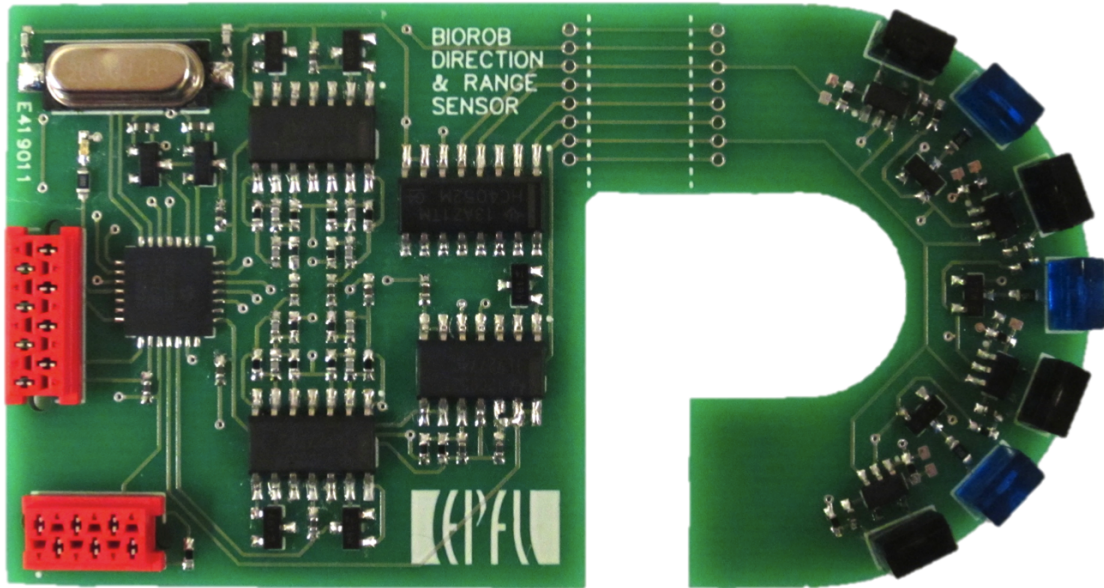


Figure 18: Second prototype of transceiver.

The second prototype transceiver included several improvements over the first revision. These include a more straightforward design, reduced number of components, reduced active board area, and Micro-MaTcH connectors for easier interfacing. It was also designed specifically to work with the *Salamandra robotica*. The board is designed as two, separable components. The first is the array of detectors and transmitters that can be placed on the head of the robot. This connects to the processing board inside of the robot either directly through the PCB or, once the components have been separated, through a shielded Belden 9537 cable. The second component, which contains the filter chain and processing, is designed to interface directly with the main processing board in the head of the *Salamandra robotica*. For this revision, the schematics were significantly updated and layout was again done by hand. Design changes include simplified peak detectors to allow for easier resetting and the use of a multiplexer instead of an analog switch to prevent accidental connection of multiple detectors (the multiplexer guarantees break-before-make connections).

5 Results

We performed a series of tests with the prototype hardware to characterize the system. Unfortunately, due to time constraints (manufacturing delays), not all of the desired tests were performed. This section discusses our preliminary results and proposes some new experiments.

5.1 Distance calibration

The first step toward verifying the system was ensuring that we could get accurate distance information from the device. For this test, one prototype acted as a transmitter

while another served as the receiver. The transmitter emitted a constant 10 kHz signal (square wave) on three TSKS5400 infrared emitters. Each emitter had an 24 mA “on” current (34 mW), resulting in an average power emission of 17 mW per emitter. We considered only a single detector that was in line with one of the emitters. Measurements were taken on the signal level after the multiplexer (AC-coupling only) and after the 4 filter stages. This information was sent to the computer via a serial connection. The transmitter was slowly moved away from the receiver and measurements were recorded at one centimeter increments for 1.2 meters (as measured by hand). Fifty measurements were taken at each distance and averaged to find the typical signal level at each stage for a given distance. Figure 19 shows the results of this experiment.

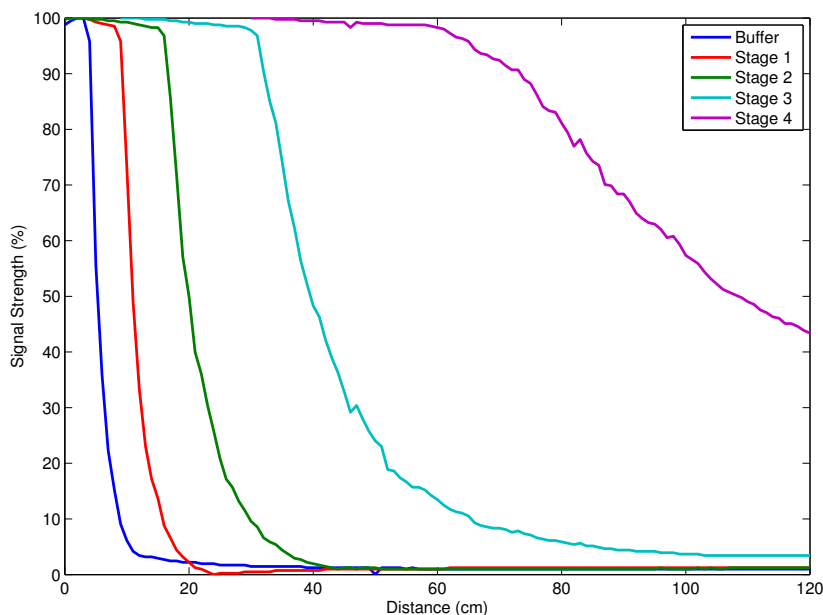


Figure 19: Graph showing the signal strength at each point along the filter chain with an aligned transmitter.

We see a very strong correlation between distance and signal strength. We also note how the filter chain increases the dynamic range of the sensor: as one filter stage loses sensitivity, another becomes active. By actively adjusting the stage of interest, we can continuously get precise sensor data, regardless of the perceived signal level. Using this data, we can create an empirical relationship between signal strength and distance. This test only characterized the sensor’s response for a very low power transmitter, resulting in a limited range of under 2 meters. We can greatly increase the range by using more or higher power emitters (note that the system would have to be recalibrated to the new signal levels). Increasing the number of emitters can also have the positive effect of creating a more uniform emission from the transmitter. It would be interesting to perform tests using a stronger transmitter and further examine the possibility of using visible light for improved underwater performance. Both of these would require a similar calibration process, though on difference scales.

5.2 Angle determination

Initial testing of angle determination was performed by moving the transmitter in front of the sensor and observing the effect on the signal chain. A first order positioning system was created by assuming that the signals direction is simple the angle of the detector which returns the shortest range (strongest signal). This gives strong performance, but only narrows the signal to a 45° area. We also lose much of the distance information by only using one sensor. A better solution uses multiple detectors and their angular sensitivity profiles to intelligently estimate the position and range. An examples of such systems can be found in [48, 49]. Further tests to characterize the angular sensitivity of the detectors should be performed and incorporated to improve the results.

5.3 Reflective obstacle sensing

We performed some qualitative tests to examine the sensor's effectiveness as an obstacle detection sensor. For these tests, we transmitted signals using the onboard transmitter and looked for reflected signals on the detectors. The position of the activated detector can provide information on the position of the obstacle and the amount of reflected light is related to the distance of the object. On their own, the detectors are overly sensitive to the light from the emitters that are reflected out the sides of the TSKS5400 casing. These internal reflections cause the sensor to nearly saturate the signal strength readings even before obstacles are introduced. Realizing this and ignoring the high baseline signal, we can detect obstacles within a range of approximately 1 cm. This allows the sensor to be useful for detecting collisions, but little else.

In order to minimize the signal from neighboring transmitters, we used a cardboard separator to block crosstalk. This greatly improved the sensor's performance. We saw a usable range of several centimeters (5+ cm). The performance could be even further improved by using higher quality separators or by placing the emitters and detectors on opposite sides of the printed circuit board. This improved separation lowers the baseline signals level and increases the sensitivity to the reflected light. The reflected signal levels could then be calibrated and used. Note, however, that the distance measurements will then be sensitive to objects' absorption of the wavelength of light being used (objects which absorb the wavelength will appear father than they really are).

5.4 Communication

Only very limited tests were done to measure the communication ability of the sensor. In particular, pulse width modulation (PWM) was applied on top of the 10 kHz carrier. The receiver would simply measure how many readings in a row it observed a signal above a certain strength before it was lost. The amount of time a signal is perceived corresponds the the pulse width. This proof of concept, chosen for ease of implementation, worked but is far from the most effective solution. Better solutions would use more precise timing and may even separate the sending of data from the signal strength measurement, allowing for much higher data rates.

6 Conclusion and future work

This paper outlines the design of a relative localization system for mobile robots. The final prototype hardware can get range and bearing information, along with data from a modulated transmitter. It integrates with the *Salamandra robotica*, is smaller than existing systems, and is highly adaptable (just as functional using visible light emitters and detectors). Currently, the range and bearing information is quite rough, but this can be improved with further testing and calibration. A higher power transmitter would increase the range of the sensor and improved firmware could greatly enhance communication ability.

References

- [1] Govind P Agrawal. Optical Communication Systems. 2005.
- [2] Davide Anguita, Davide Brizzolara, and Giancarlo Parodi. Design and Implementation of HDL Modules and Circuits for Underwater Optical Wireless Communication. *Language*.
- [3] Davide Anguita, Davide Brizzolara, and Giancarlo Parodi. Prospects and Problems of Optical Diffuse Wireless Communication for Underwater Wireless Sensor Networks (UWSNs). pages 1–26.
- [4] Davide Anguita, Davide Brizzolara, and Giancarlo Parodi. Optical Wireless Communication for Underwater Wireless Sensor Networks: Hardware Modules and Circuits Design and Implementation. *IEEE*, 2010.
- [5] Davide Anguita, Davide Brizzolara, Giancarlo Parodi, and Qilong Hu. Optical Wireless Underwater Communication for AUV : Preliminary Simulation and Experimental Results. *IEEE Oceans*, pages 1–5, 2011.
- [6] Mohammed Zishan Ansari, Shobhit Mangla, and Arijit Chattopadhyaya. Gold Code Sequences. 2008.
- [7] Marcel Babin and Dariusz Stramski. Light absorption by aquatic particles in the near-infrared spectral region. *Limnology and Oceanography*, 47(3):911–915, 2002.
- [8] Paul Barna and Steve Schlanger. Fundamentals of the Infrared Physical Layer. pages 1–12, 2004.
- [9] Kumen Blake. Op Amp Precision Design: Random Noise. pages 1–26, 2008.
- [10] Andy Britton. Simple Digital Filter Design for Analogue Engineers. (June), 2010.
- [11] Bruce Carter. A Single-Supply Op-Amp Circuit Collection. (November):1–27, 2000.
- [12] Bruce Carter. Filter Design in Thirty Seconds. (December):1–14, 2001.
- [13] Bruce Carter. More Filter Design on a Budget. (December):1–19, 2001.
- [14] Riccardo Cassinis, Fabio Tampalini, and Roberto Fedrigotti. Active markers for outdoor and indoor robot localization. *Electronics*.

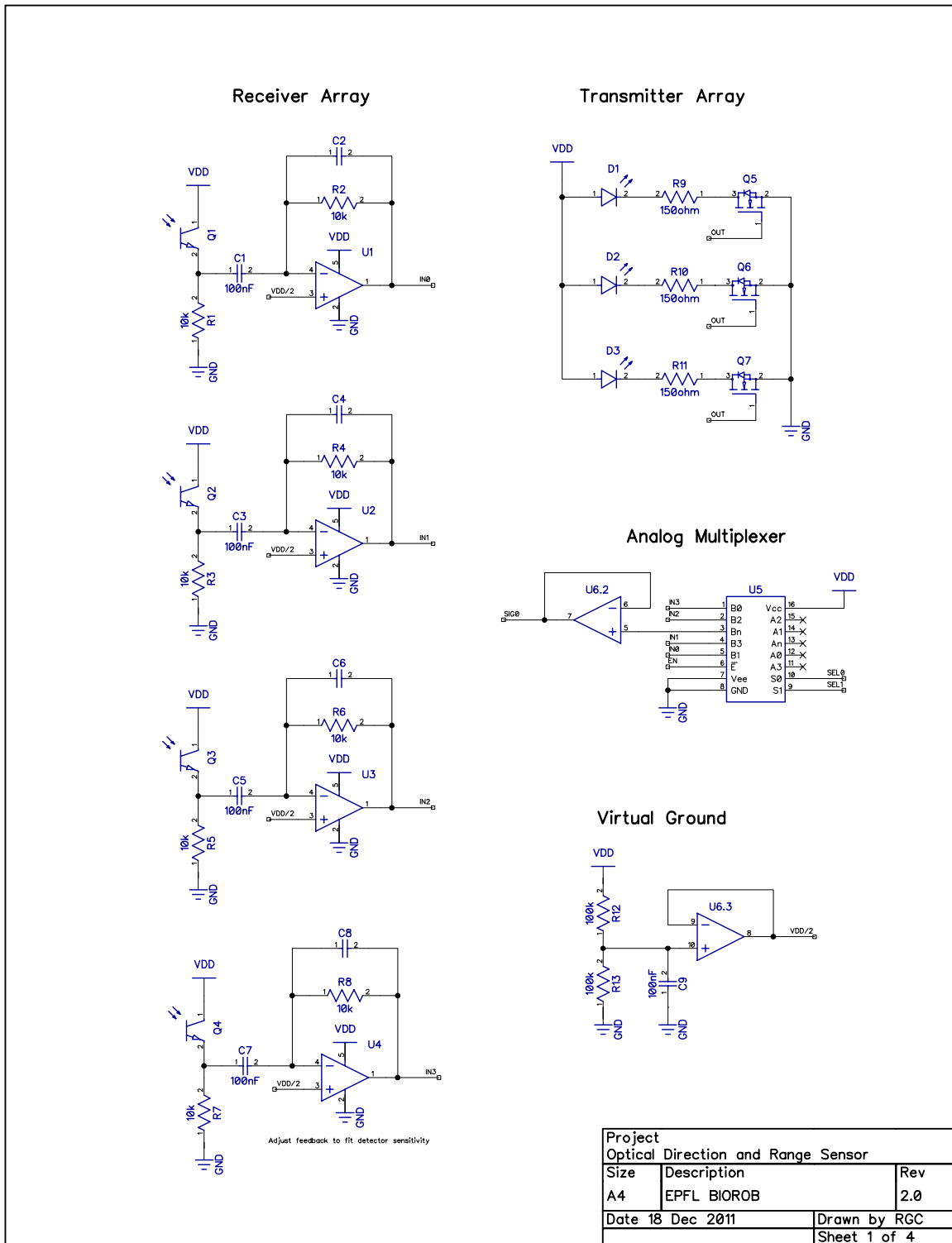
- [15] William C. Cox, Jim a. Simpson, Carlo P. Domizioli, John F. Muth, and Brian L. Hughes. An underwater optical communication system implementing Reed-Solomon channel coding. *Oceans 2008*, pages 1–6, 2008.
- [16] Alessandro Crespi. *Design and Control of Amphibious Robots with Multiple Degrees of Freedom*. PhD thesis, 2007.
- [17] Alessandro Crespi and Auke Jan Ijspeert. Salamandra robotica: A Biologically Inspired Amphibious Robot that Swims and Walks. pages 3–36, 2009.
- [18] Analog Devices. Analog Switches and Multiplexers Basics. pages 1–23, 2009.
- [19] Marek Doniec, Carrick Detweiler, Iuliu Vasilescu, and Daniela Rus. Using Optical Communication for Remote Underwater Robot Operation Robot (in water). *Artificial Intelligence*, 2010.
- [20] Harry J R Dutton. Understanding Optical Communications. *Communications*.
- [21] N. Farr, a.D. Chave, L. Freitag, J. Preisig, S.N. White, D. Yoerger, and F. Sonnichsen. Optical Modem Technology for Seafloor Observatories. *Oceans 2006*, pages 1–6, September 2006.
- [22] Z. Ghassemlooy, W.O. Popoola, S. Rajbhandari, M. Amiri, and S. Hashemi. A synopsis of modulation techniques for wireless infrared communication. *2007 ICTON Mediterranean Winter Conference*, pages 1–6, 2007.
- [23] a. Gutierrez, a. Campo, M. Dorigo, J. Donate, F. Monasterio-Huelin, and L. Magdalena. Open E-puck Range & Bearing miniaturized board for local communication in swarm robotics. *2009 IEEE International Conference on Robotics and Automation*, pages 3111–3116, May 2009.
- [24] Alvaro Gutiérrez, Alexandre Campo, Marco Dorigo, Daniel Amor, Luis Magdalena, and Félix Monasterio-Huelin. An Open Localization and Local Communication Embodied Sensor. *Sensors*, 8(11):7545–7563, November 2008.
- [25] Frank Hanson and Stojan Radic. High bandwidth underwater optical communication. *Applied optics*, 47(2):277–83, January 2008.
- [26] Sean Hoyt, Sam Mckennoch, Linda G Bushnell, and Linda Bushnell. An Autonomous Multi-Agent Testbed using Infrared Wireless Communication and Localization. (206), 2005.
- [27] Steve Hranilovic. Wireless Optical Communication Systems. *Communications*, 4530(2001):27–35, 2004.
- [28] Stuart Williams Iain Millar, Martin Beale, Bryan Donoghue, Kirk Lindstrom. The IrDA Standards for High-Speed Infrared Communications. January 1998.
- [29] Auke Jan Ijspeert, Alessandro Crespi, Dimitri Ryczko, and Jean-Marie Cabelguen. From swimming to walking with a salamander robot driven by a spinal cord model. *Science (New York, N.Y.)*, 315(5817):1416–20, March 2007.

- [30] Texas Instruments. FSK Modulation and Demodulation With the MSP430 Microcontroller Application Report. 1998.
- [31] Yousuke Ito, Shinichiro Haruyama, and Masao Nakagawa. Short-Range Underwater Wireless Communication Using Visible Light LEDs. *System*, pages 1–24.
- [32] J.M. Kahn and J.R. Barry. Wireless infrared communications. *Proceedings of the IEEE*, 85(2):265–298, 1997.
- [33] Joseph M Kahn. Modulation and Detection Techniques for Optical Communication Systems. *Lightwave*, 2(M):2–4, 2006.
- [34] Ian Kelly and Alcherio Martinoli. A scalable, on-board localisation and communication system for indoor multi-robot experiments. *Sensor Review*, 24(2):167–180, 2004.
- [35] Jurgen Kemper and Holger Linde. Challenges of passive infrared indoor localization. *2008 5th Workshop on Positioning, Navigation and Communication*, 2008:63–70, March 2008.
- [36] K H Kim, H D Choi, S Yoon, K W Lee, H S Ryu, C K Woo, and Y K Kwak. Development of Docking System for Mobile Robots Using Cheap Infrared Sensors. *Electronics*, pages 287–291, 2005.
- [37] Markus Kuhn. Digital Signal Processing. 2009.
- [38] Sooyong Lee. Use of infrared landmark zones for mobile robot localization. *Industrial Robot: An International Journal*, 35(2):153–159, 2008.
- [39] Emanuele Lopelli, J D Van Der Tang, and A H M Van Roermund. FSK Demodulator Topologies for Ultra-low Power Wireless Transceivers. pages 241–246.
- [40] F.J. Lopez Hernandez, E. Poves, R. Perez-Jimenez, and J. Rabadan. Low-Cost Diffuse Wireless Optical Communication System based on White LED. *2006 IEEE International Symposium on Consumer Electronics*, pages 1–4, 2006.
- [41] Feng Lu, Sammy Lee, Jeffrey Mounzer, and Curt Schurgers. Short Paper : Low-Cost Medium-Range Optical Underwater Modem. *Computer Engineering*, pages 3–6, 2009.
- [42] Ron Mancini. Op Amps For Everyone. (August), 2002.
- [43] Arpit Mehta. High-Speed Op Amp Enables Infrared (IR) Proximity Sensing. 2009.
- [44] H. Melchior, M.B. Fisher, and F.R. Arams. Photodetectors for optical communication systems. *Proceedings of the IEEE*, 58(10):1466–1486, 1970.
- [45] Jim Partan, Jim Kurose, and Brian Neil Levine. A survey of practical issues in underwater networks. *ACM SIGMOBILE Mobile Computing and Communications Review*, 11(4):23, October 2007.
- [46] Khoman Phang. CMOS Optical Preamplifier Design Using Graphical Circuit Analysis. *Computer Engineering*, 2001.

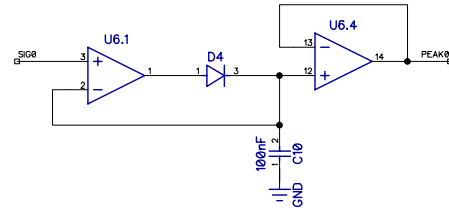
- [47] Robin M Pope and Edward S Fry. Absorption spectrum (380-700 nm) of pure water. II. Integrating cavity measurements. *Applied Optics*, 1997.
- [48] J. Pugh and A. Martinoli. Relative localization and communication module for small-scale multi-robot systems. *Proceedings 2006 IEEE International Conference on Robotics and Automation, 2006. ICRA 2006.*, pages 188–193, 2006.
- [49] J. Pugh, X. Raemy, C. Favre, R. Falconi, and a. Martinoli. A Fast Onboard Relative Positioning Module for Multirobot Systems. *IEEE/ASME Transactions on Mechatronics*, 14(2):151–162, April 2009.
- [50] R. Ramirez-Iniguez. Indoor optical wireless communications. *IEE Colloquium Optical Wireless Communications*, 1999:14–14, 1999.
- [51] Frederic Rivard, Jonathan Bisson, Francois Michaud, and Dominic Letourneau. Ultrasonic relative positioning for multi-robot systems. *2008 IEEE International Conference on Robotics and Automation*, pages 323–328, May 2008.
- [52] C Robert, P Tomé, C Botteron, P Farine, R Merz, and A Blatter. Low Power ASIC transmitter for UWB-IR radio communication and positioning. *Pulse*, 2(September):15–17, 2010.
- [53] James F. Roberts, Timothy S. Stirling, Jean-Christophe Zufferey, and Dario Floreano. 2.5D Infrared Range and Bearing System for Collective Robotics. *2009 IEEE/RSJ International Conference on Intelligent Robots and Systems*, pages 3659–3664, October 2009.
- [54] S.I. Roumeliotis and G.a. Bekey. Distributed multirobot localization. *IEEE Transactions on Robotics and Automation*, 18(5):781–795, October 2002.
- [55] R. E. Saad. Proximity Sensing for Robotics. 1999.
- [56] Felix Schill, Uwe R Zimmer, and Jochen Trumpf. Visible Spectrum Optical Communication and Distance Sensing for Underwater Applications. In *Proceedings of ARCA 2004*, 2004.
- [57] Vishay Semiconductors. Infrared Data Communication According to IrDA Standard. 2006.
- [58] Jim A Simpson, William C Cox, John R Krier, Brandon Cochenour, Brian L Hughes, and John F Muth. 5 Mbps Optical Wireless Communication with Error Correction Coding for Underwater Sensor Nodes. pages 6–9, 2010.
- [59] Kasper Stoy. Using Situated Communication in Distributed Autonomous Mobile Robotics.
- [60] Mohd Supa’at. *Advances in Free Space Optical Technology*. 2007.
- [61] Shuchin M. Taher and James R. Scott. A comparison of InP HBT transimpedance amplifier topologies for high dynamic range photonic links. *2009 Asia Pacific Microwave Conference*, pages 222–225, December 2009.

- [62] Maurice Tivy, Paul Fucile, and Enid Sichel. A Low Power, Low Cost, Underwater Optical Communication System. *Ridge 2000*, 1(April):27–29, 2004.
- [63] Bob Watson. FSK : Signals and Demodulation. 1980.

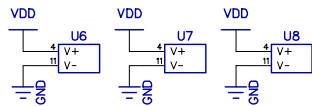
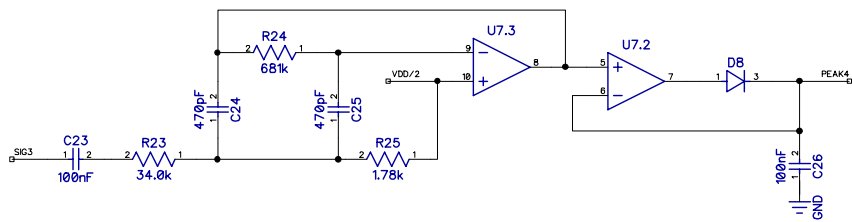
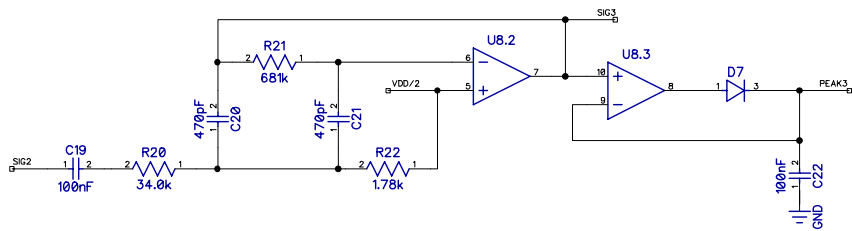
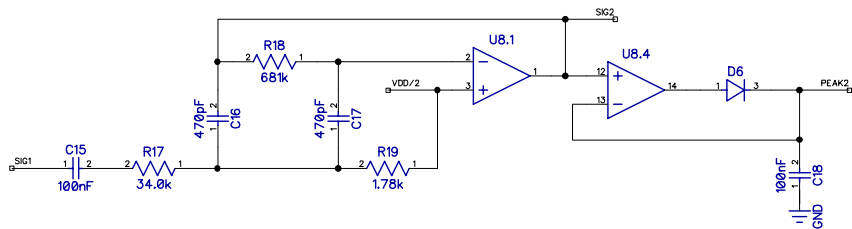
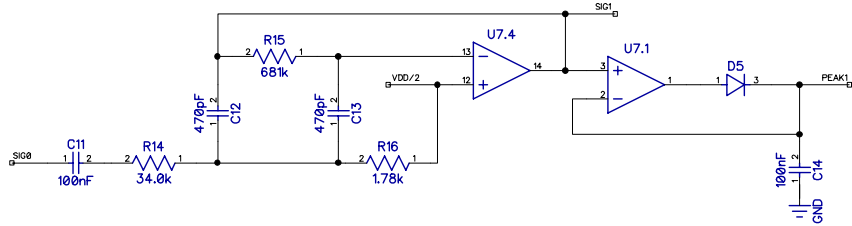
A Schematics



Peak Detectors

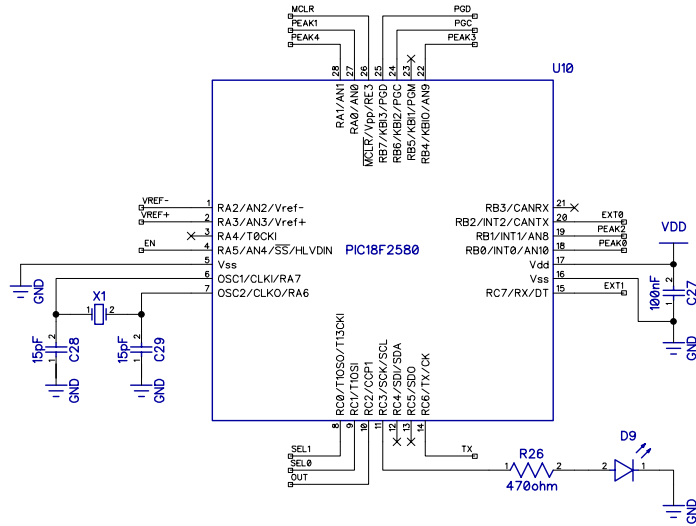


Cascaded 10 kHz Filters

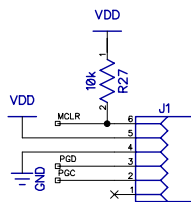


Project		
Optical Direction and Range Sensor		
Size	Description	Rev
A4	EPFL BIOROB	2.0
Date	18 Dec 2011	Drawn by RGC
		Sheet 2 of 4

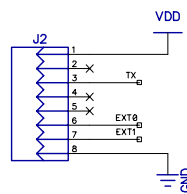
Microcontroller



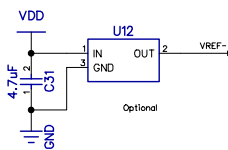
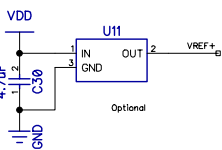
Programming Port



Interface Port



Reference Voltages



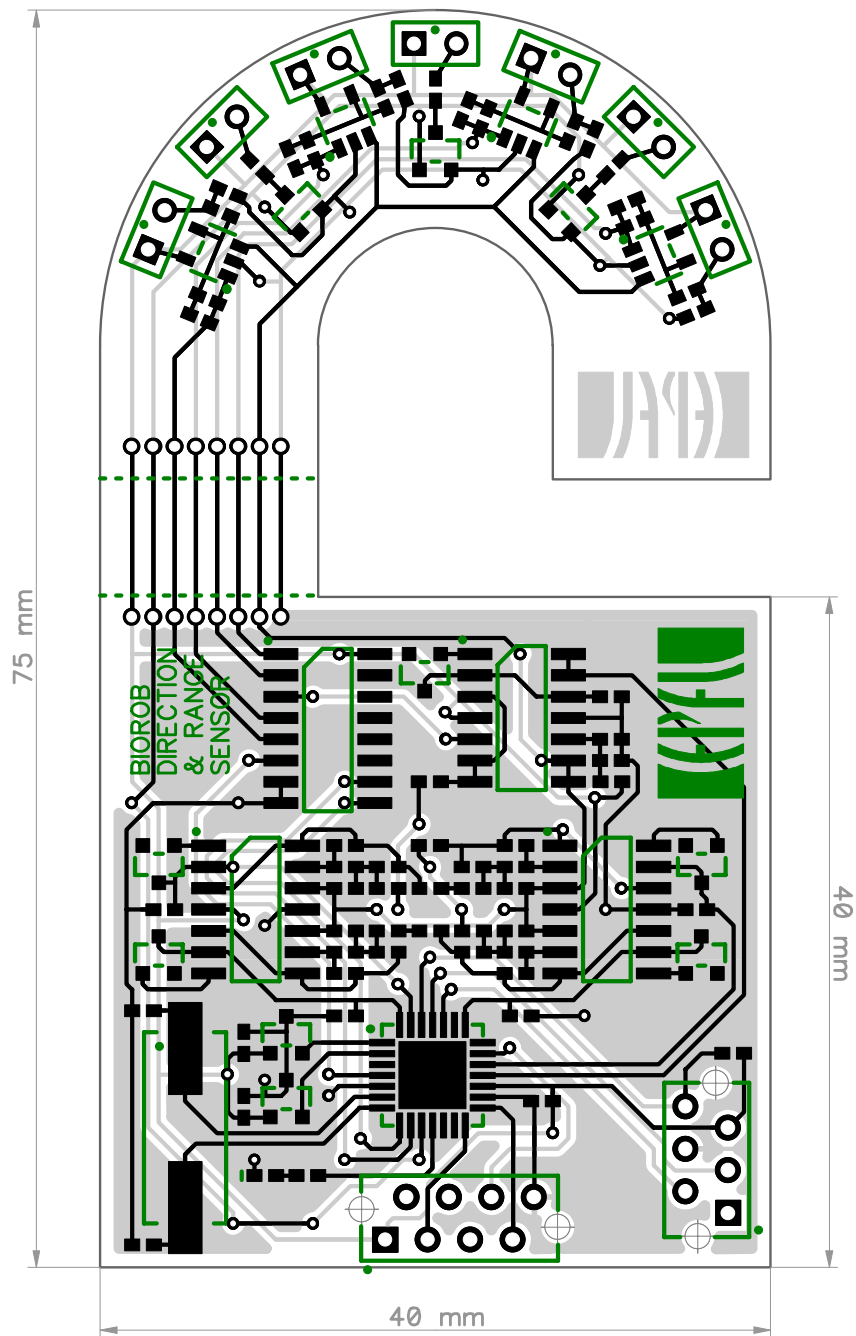
Project		
Optical Direction and Range Sensor		
Size	Description	Rev
A4	EPFL BIOROB	2.0
Date	18 Dec 2011	Drawn by RGC
Sheet 3 of 4		

Bill of Materials

Type	RefDes	Pattern	Quantity
100nF CAP	C1, C3, C5, C7, C9-11, C14-15, C18-19, C22-23, C26-27	0402	15
470pF CAP	C12-13, C16-17, C20-C21, C24-25	0402	8
FEEDBACK CAP	C2, C4, C6, C8	0402	4
15pF CAP	C28-29	0402	2
4.7uF CAP	C30-31	0402	2
TSKS5400	D1-3	SIDE-LENS	3
BAS16	D4-8	SOT-23	5
LED	D9	0402	1
MICRO-MATCH 215079-6	J1	MM6	1
MICRO-MATCH 215464-8	J2	MM8	1
TEKT5400	Q1-4	SIDE-LENS	4
2N7002	Q5-7	SOT-23	3
10k RES	R1-8, R27	0402	9
150ohm RES	R9-11	0603	3
470ohm RES	R26	0402	1
100k RES	R12-13	0402	2
34.0k RES	R14, R17, R20, R23	0402	4
681k RES	R15, R18, R21, R24	0402	4
1.78k RES	R16, R19, R22, R25	0402	4
TLV2771	U1-4	SOT-23-5	4
PIC18F2580	U10	QFN28	1
VOLTAGE REF	U11-12	SOT-23	2
CD74HC4052	U5	S016	1
TLV2774	U6-8	S014	3
CRYSTAL HC49	X1	HC49	1

Project		
Optical Direction and Range Sensor		
Size	Description	Rev
A4	EPFL BIOROB	2.0
Date	18 Dec 2011	Drawn by RGC
		Sheet 4 of 4

B Printed circuit board



C Datasheets

C.1 TSKS5400

<http://www.vishay.com/docs/83780/tsks5400.pdf>

C.2 TEKT5400

<http://www.vishay.com/docs/81569/tekt5400.pdf>

C.3 CD74HC4052

<http://www.ti.com/lit/ds/symlink/cd74hc4052.pdf>

C.4 TLV2774/2

<http://www.ti.com/lit/ds/symlink/tlv2774.pdf>

C.5 BAS16

http://www.nxp.com/documents/data_sheet/BAS16_SER.pdf

C.6 2N7002

http://www.nxp.com/documents/data_sheet/2N7002.pdf